Piotr KURGAN, Sławomir KOZIEŁ

Gdańsk University of Technology, Faculty of Electronics, Telecommunications and Informatics

doi:10.15199/48.2016.09.18

On Fast Optimization of Quasi-Periodic Slow-Wave Structures: Application to Broadband Microwave Coupler Miniaturization

Abstract. *This work discusses design optimization of quasi-periodic slow-wave structures in the context of wideband branch-line coupler miniaturization. Size reduction is achieved by using slow-wave structures as substitutes for conventional transmission lines that constitute a reference circuit. Selection of a specific cell realization as well as determination of a repetition factor of the quasi-periodic slow-wave structure is accomplished by optimization-based theoretical studies. The principal design procedure involves cell optimization using electromagnetic simulations, local response surface approximation modeling of the single cell, and surrogate-based optimization of the slow-wave structure composed of cascaded cell approximation models. Surrogate-based design closure is applied to account for T-junction effects neglected throughout the design process. The final coupler exhibits a high-performance operation over a 31% bandwidth and occupies only 1/3 of the reference circuit area.*

Streszczenie. *W pracy omówiono problem optymalizacji quasi-periodycznych struktur ze spowolnieniem fali w kontekście miniaturyzacji szerokopasmowego sprzęgacza gałęziowego. Redukcja powierzchni została osiągnięta poprzez zastosowanie struktur ze spowolnieniem fali jako zamienników dla konwencjonalnych linii transmisyjnych, które są podstawowymi elementami składowymi obwodu referencyjnego. Połączenie kaskadowe kilku komórek ze spowolnieniem fali umożliwia uzyskanie szerokiego pasma pracy kompletnej struktury. Wybór konkretnej realizacji komórki oraz określenie współczynnika powtarzalności dla quasi-periodycznej struktury ze spowolnieniem fali jest przeprowadzone na podstawie badań teoretycznych opartych na optymalizacji. Właściwa procedura projektowania wykorzystuje optymalizację elektromagnetyczną pojedynczej komórki oraz jej lokalne modelowanie aproksymacyjne, a następnie metodę modeli zastępczych do przeprowadzenia efektywnej optymalizacji kaskadowego połączenia lokalnych modeli aproksymacyjnych pojedynczej komórki. Ponadto zastosowano efektywną procedurę strojenia sprzęgacza gałęziowego w celu uwzględnienia efektów łączników typu T. Otrzymana w ten sposób struktura cechuje się wysoką wydajnością oraz pracą szerokopasmową przy zajmowanej powierzchni odpowiadającej 1/3 powierzchni struktury referencyjnej. (**Na temat szybkiej optymalizacji quasi-periodycznych struktur ze spowolnieniem fali. Miniaturyzacja szerokopasmowego sprzęgacza mikrofalowego**).*

Keywords: broadband branch-line couplers, microwave circuit miniaturization, response surface approximation, simulation-driven design, surrogate-based optimization, space mapping.
Słowa kluczowe: szerokopasmowe sprzęgacze gałęziowe, miniaturyzacja układów mikrofalowych, aproksymacja odpowiedzi, symulacyjne metody projektowania, metoda modeli zastępczych, odwzorowanie przestrzeni.

Introduction

Miniaturization of distributed-element passive circuits is an important topic of contemporary microwave engineering [1]–[6]. The currently prevailing approach to circuit size reduction is based on decomposition of a conventional circuit and subsequent replacement of its building blocks with so-called slow-wave structures, whose role is to approximate the characteristics of their conventional counterparts, while offering an increased electrical length to physical length ratio [5], [6]. Slow-wave structures are typically realized as intricate combinations of high-impedance strips and low-impedance stubs or line sections [5], which embody the concept of spatially separated storage of magnetic and electric energy of [7]. The fundamental difficulty when applying this miniaturization method is a dramatic increase of design problem complexity, including high cost of electromagnetic (EM) analysis, lack of accurate theory-based models, and multi-dimensional search spaces [6]. The problem becomes even more pronounced when designing compact microwave circuits for wideband applications. This often requires the use of quasi-periodic slow-wave structures instead of single-element ones that are inherently narrowband [3], [5]. The former are even more CPU-intensive than the latter, which is a limiting factor for obtaining feasible EM-driven design methodologies for compact microwave circuit with wideband characteristics.

State-of-the-art strategies for the development of compact microwave circuits almost exclusively consider design problems of narrowband components, miniaturized by means of single-element slow-wave structures [1], [4], [6]. Majority of them apply transmission line (TL) theory to provide closed-form design formulas for the target devices, but require some sort of EM-based fine-tuning procedure to account for inaccuracies of the utilized models [1], [2], [4]. Design closure is typically realized using repetitive parameter sweeps or direct optimization, both being computationally expensive. This difficulty can be alleviated through surrogate-based optimization (SBO) [8], which relies on iteratively corrected fast low-fidelity models (surrogates) replacing high-fidelity EM models. One should note that SBO techniques such as space mapping (SM) [9] indispensably require low-fidelity models to be well-aligned with their high-fidelity counterparts. Development of such models for quasi-periodic slow-wave structures is an extremely challenging task due to limitations of TL theory in modeling of complex cross-coupling effects between adjacent slow-wave cells [6], [10].

This work presents a customized procedure for the construction of a reliable surrogate model pertaining to a quasi-periodic slow-wave structure. The proposed approach involves low-cost EM simulations, local approximation modeling, space mapping and surrogate-based optimization to provide accurate results. Demonstration example is provided.

Case Study: Wideband compact Branch-Line Coupler

Here, we introduce the structure of a wideband branch-line coupler (BLC) and formulate its miniaturization-oriented design problem. Preliminary studies on quasi-periodic slow-wave structures based on equivalent circuit models and numerical optimization are also included.

Reference Structure

Hybrid branch-line couplers (BLCs) are vital microwave components widely used in balanced-type applications to provide an equal power split between the output ports with a 90° phase shift [11]. A conventional single-section BLC exhibits a narrow bandwidth of about 10% [11], which can be overcome by increasing the number of coupler sections [11], [12].

Consider a standard two-section BLC model of Fig. 1(a), composed of seven quarter-wavelength TLs of Z_1–Z_3 impedances. Practical figures of merit for couplers with a

wideband operation include (i) fractional bandwidth (BW), defined here as symmetrical—with respect to the center frequency f_0—intersection of the return loss $|S_{11}|$ and isolation $|S_{41}|$ that remain below the level of –20 dB, and (ii) $\mathrm{d}S$, denoting the absolute difference between the transmission $|S_{21}|$ and coupling $|S_{31}|$ at f_0. For illustration purposes, we use these quantities to evaluate conventional design solutions of the Butterworth and Chebyshev [12] type (see Fig. 2(b)). Both designs exhibit non-zero $\mathrm{d}S$ which is a deviation from the desired performance. Also, different ranges of circuit operation are observed, where the higher BW corresponds to the higher $\mathrm{d}S$. To address this issue, the BLC model of Fig. 1(a) is optimized to obtain a possibly maximum BW together with an equal power split between the output ports at f_0, i.e., $\mathrm{d}S$ = 0. For simplification, the number of optimization variables is reduced using the substitution of $Z_3 = Z_1$.

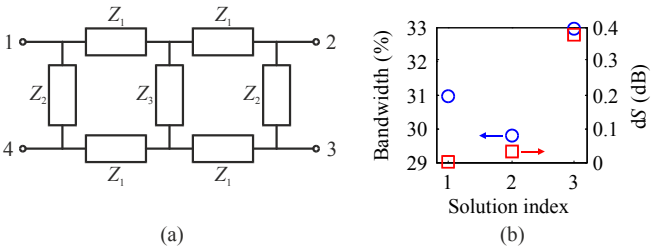

Fig. 1. (a) Two-section BLC model (each TL is 90° at f_0); (b) BW (blue circle) and $\mathrm{d}S$ (red square) for three design solutions: 1 – optimization-based (Z_1 = 34.6 Ω, Z_2 = 118.2 Ω, $Z_3 = Z_1$), 2 – Butterworth (Z_1 = 36.3 Ω, Z_2 = 120.5 Ω, Z_3 = 37.2 Ω), 3 – Chebyshev (Z_1 = 26.9 Ω, Z_2 = 105.2 Ω, Z_3 = 24.3 Ω)

Practical considerations impose that the widths of physically realized TLs are constrained by fabrication limitations and slow-wave structure design restrictions. Specifically, we assume that the lower and upper limits of microstrip TL realization are 0.1 mm and 3.25 mm, respectively. For the selected substrate (here, TLC-32 of ε_r = 3.2 and h = 0.787 mm), the available impedance range is 34.6 Ohm to 166 Ohm. The optimization task of the reference BLC is formulated as:

$$\boldsymbol{x}_{ref}^{*} = \arg\min_{x}\left\{-BW(\boldsymbol{x};f) + \beta\cdot\left[\mathrm{d}S(\boldsymbol{x};f_0)/0.1\right]^2\right\} \quad (1)$$

where $\boldsymbol{x}_{ref} = [Z_1\ Z_2]^T$ is a vector of adjustable impedances of the circuit; $BW(\boldsymbol{x};f)$ and $\mathrm{d}S(\boldsymbol{x};f_0)$ are the fractional bandwidth and the transmission-coupling imbalance at f_0, respectively.

Solving (1) with the penalty factor set to $\beta = 10^4$ permits maximization of BW while enforcing $\mathrm{d}S$ = 0; $\boldsymbol{x}_{ref}^{*}$ = [34.6 118.16]^T Ohm is the optimized design solution obtained at a negligible CPU cost. The first variable being at its lower bound suggests that further bandwidth increase is possible; however, lowering of this impedance would lead to implementational issues of slow-wave TLs [5]. A practical realization of the optimized model outperforms conventional designs by providing an ideal power split at f_0 together with a 31% BW. When designed for f_0 = 1 GHz using the above dielectric substrate, it occupies an excessively large area of 93.23 mm × 51.17 mm, which calls for applying an efficient miniaturization procedure.

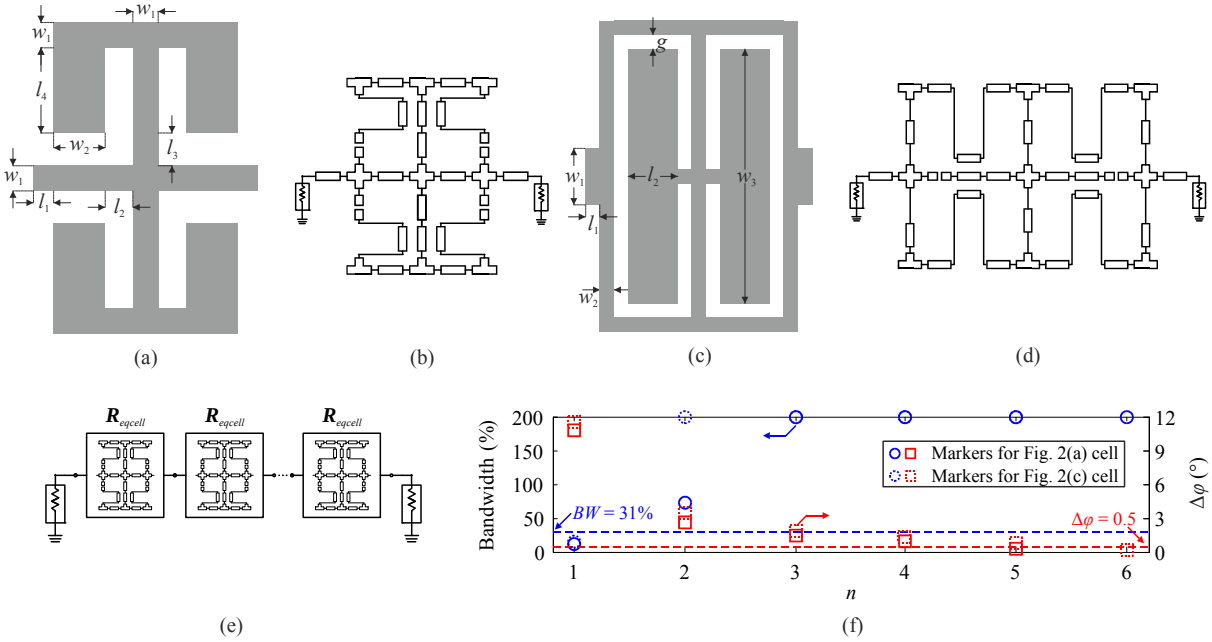

Fig. 2. (a) Parameterized layout of a T-shaped cell, and (b) its equivalent circuit; (c) Dumbbell-shaped cell layout with (d) its corresponding low-fidelity model; (e) Recurrent network of an n-element cascade of cell models $\boldsymbol{R}_{eq.cell}$; (f) Comparison of n-element slow-wave cell cascades: BW (blue circle) and absolute phase difference between a conventional TL and a given n-element cascade (red square)

Quasi-Periodic Slow-Wave Structure

The BLC of Section 2.1 is composed of high- and low-impedance TLs that require length diminution for circuit size reduction. The high-impedance strips can be shortened by folding [5], [13]. On the other hand, the abbreviation of low-impedance line sections can be accomplished by using quasi-periodic structures that feature a slow-wave effect. However, selection of a suitable slow-wave structure geometry from numerous physical realizations available in the literature (e.g., [5]), as well as determination of the proper number n of elements (so-called cells) forming a quasi-periodic slow-wave structure is still an open issue. Here, this is done by a simple optimization-based comparative analysis of two example slow-wave structures. We illustrate this

concept with slow-wave cells of Figs. 2(a) and 2(c), whose geometries are described by the vectors $\boldsymbol{x}_{cell}$ = [l_1 l_2 l_3 l_4 w_1 w_2]^T, and $\boldsymbol{x}_{cell}$ = [l_1 l_2 w_1 w_2 w_3 g]^T, respectively. The network models of Figs. 2(b) and 2(d) allow us to find the smallest number n of elements in the cascade, so that BW of the respective recurrent network of Fig. 2(e) is at least 31%, and the absolute difference between the transmission phase of a conventional TL and n-element cascade, $\Delta\varphi$, is less than ε = 0.5°. The task is to compare n-element cascades of cell circuit models (n = 1, 2, …), each optimized using ADS [14] to obtain a required phase shift at f_0, arg(S_{21}) = ϕ_c= –90°/n, and to minimize the return loss $|S_{11}|$ at f_0 with ports of 34.6 Ohms. The process is realized independently for each cell. Thus, the cell optimization task is defined as:

$$\boldsymbol{x}_{cell}^{*} = \arg\min_{\boldsymbol{x}} \left\{ \max_{f=f_0} |S_{11}(\boldsymbol{x};f)| + \beta \cdot \left[\arg(S_{21}(\boldsymbol{x};f_0)) - \phi_c \right]^2 \right\} \quad (2)$$

where $S_{11}(x;f)$ and $S_{21}(x;f)$ denote explicit dependence of S-parameters on frequency; as before, $\beta = 10^4$. The family of resulting quasi-periodic slow-wave structures is compared w.r.t. the above figures of merit. The inspection of Fig. 2(f) reveals that the first condition excludes only the case of n = 1. This conclusion holds for both considered slow-wave cells. Note that for higher n, the bandwidth—which is defined as being symmetrical around f_0—can only reach the maximum value of 200%. Considering the second condition for the cell of Fig. 2(a), it can be observed that the smallest n, for which $\Delta\varphi$ stays below 0.5° in the entire bandwidth, is five. For the cell of Fig. 2(c), the second condition is satisfied by n = 6. Thus, we select the first slow-wave cell in a five-element configuration for the following rapid design optimization procedure. The optimized equivalent circuit solution for n = 5 becomes the starting point for the subsequent design process: $x_{cell}^{(0)}$ = [0.41 0.12 0.14 3.15 0.38 1.78]^T mm.

Design Procedure

Here, an efficient design procedure of compact wideband BLCs is presented. Due to their modular architecture, the BLC design problem can be simplified to the development of their individual building blocks. Rapid design closure of [6] may be applied afterwards to account for T-junction effects or other phenomena omitted during earlier stages. For the sake of efficiency and reliability, we use sparsely sampled EM simulation data, response surface approximations (RSAs), and space mapping (SM) as a fundamental tool of model correction.

Slow-Wace Cell Optimization

For accuracy, modelling of the slow-wave cells is realized using full-wave EM analysis, implemented in Sonnet ***em*** [15]. This is feasible, as the cell model is relatively cheap even with 0.01 × 0.01 mm grid and fine meshing (~ 1 min/freq.) as opposed to the cascade (~10 min/freq.) or compact BLC (~5 hour/freq.). The problem (2) is solved directly using a pattern search algorithm (cf. [8]). The target phase shift is ϕ_c= –18° given a five-cell setup for constructing the 90-degree TL of 34.6-ohm impedance. The lower/upper bounds $\boldsymbol{l}$/$\boldsymbol{b}$ of the search space are given by $\boldsymbol{l}$ = [0.05 0.1 0.1 0.1 0.1 0.1]^T mm, and $\boldsymbol{u}$ = [1 1 1 5 0.5 5]^T mm. The EM model evaluated at the initial point $\boldsymbol{x}_{cell}^{(0)}$ returns $|S_{11}|$ = –25.2 dB, and arg(S_{21}) = –23.9° at f_0, while the final solution, obtained after ~100 EM simulations, $\boldsymbol{x}_{cell}^{*}$=[0.16 0.14 0.13 3.93 0.42 1.15]^T mm, yields $|S_{11}|$ = –59.5 dB, and arg(S_{21}) = –18.0° at f_0. The high-impedance folded TL is simply designed by (2) assuming ϕ_c= –90°.

Tuning of Quasi-Periodic Slow-Wave Structure

Surrogate-based optimization (SBO) [8], used here for a feasible and reliable cascade tuning, requires a fast and well-aligned surrogate model. It is obtained from the coarse model $\boldsymbol{R}_{c.cas}$ which is developed by cascading the local RSA models $\boldsymbol{R}_{c.cell}$ of the individual slow-wave cell, constructed in the vicinity of its optimum design. More specifically, $\boldsymbol{R}_{c.cell}$ is defined around $\boldsymbol{x}_{cell}^{*}$, in the interval [$\boldsymbol{x}_{cell}^{*} - d\boldsymbol{x}$, $\boldsymbol{x}_{cell}^{*} + d\boldsymbol{x}$]. It is developed at the cost of 2m + 1 EM simulations at $\boldsymbol{x}_{cell}^{(0)} = \boldsymbol{x}_{cell}^{*}$ and at the perturbed designs $\boldsymbol{x}_{cell}^{(k)}$ = [$x_{cell.1}^{*}$ … $x_{cell.\lceil k/2 \rceil}^{*}$ + $(-1)^k dx_{\lceil k/2 \rceil}$ … $x_{cell.m}^{*}$]^T, k = 1, …, 2m, where $x_{cell.k}^{*}$ and dx_k are kth components of the vectors $\boldsymbol{x}_{cell}^{*}$ and $d\boldsymbol{x}$, respectively. $\boldsymbol{R}_{c.cell}(\boldsymbol{x})$ is a second-order polynomial without mixed terms

$$\boldsymbol{R}_{c.cell}(\boldsymbol{x}) = c_0 + \sum_{k=1}^{n} c_k x_k + \sum_{k=1}^{n} c_{n+k} x_k^2 \quad (3)$$

The parameters c_k in (3) are identified by solving the linear regression problems

$$\boldsymbol{R}_{c.cell}(\boldsymbol{x}_c^{(i)}) = \boldsymbol{R}_{f.cell}(\boldsymbol{x}_c^{(k)}), \quad k = 0,1,...,2m \quad (4)$$

where $\boldsymbol{R}_{f.cell}$ denotes an EM model of the cell. The cascade tuning is necessary, because $\boldsymbol{R}_{c.cas}$ does not account for cross-coupling effects between the cells. This is evident considering cascade performance at the initial point, $\boldsymbol{x}_{cas}^{(0)} = \boldsymbol{x}_{cell}^{*}$, evaluated by means of the EM solver [15], which gives $|S_{11}|$ = –40.9 dB, and arg(S_{21}) = –83.8° at f_0. This may be addressed by the following SBO process [8]

$$\left[\boldsymbol{x}_{cas}^{(i+1)}, l_{TL}^{(i+1)} \right] = \arg\min_{\boldsymbol{x}, l_{TL}} U\left(\boldsymbol{R}_{s.cas}^{(i)}(\boldsymbol{x}), \boldsymbol{R}_{f.TL}^{(i)}(l_{TL}) \right) \quad (5)$$

where $\boldsymbol{x}_{cas}^{(i)}$, and $l_{TL}^{(i)}$, i = 0, 1, …, approximate the solution to the cascade design problem [$\boldsymbol{x}_{cas}^{*}$,l_{TL}^{*}] = argmin{$\boldsymbol{x}$: $U_c(\boldsymbol{R}_{f.cas}(\boldsymbol{x}), \boldsymbol{R}_{f.TL}(l_{TL}))$} ($l_{TL}$ being the length of a conventional TL of 34.6-ohm impedance added at both ends of the cascade as an additional degree of freedom in phase compensation). Design specs, i.e., minimal $|S_{11}|$, and arg(S_{21}) = –90° at f_0 are encoded in U_c function. $\boldsymbol{R}_{f.TL}^{(i)}$ is a cheap EM model of a low-impedance TL. $\boldsymbol{R}_{s.cas}^{(i)}$ is the cascade surrogate model at iteration i, which corresponds to the SM-corrected [8], [9] cascade coarse model $\boldsymbol{R}_{c.cas}$

$$\boldsymbol{R}_{s.cas}^{(i)}(\boldsymbol{x}) = \boldsymbol{R}_{c.cas}(\boldsymbol{x} + \boldsymbol{q}^{(i)}) \quad (6)$$

where $\boldsymbol{q}^{(i)}$ is the input SM shift vector obtained using the usual parameter extraction procedure

$$\boldsymbol{q}^{(i)} = \arg\min_{\boldsymbol{q}} \| \boldsymbol{R}_{f.cas}(\boldsymbol{x}_{cas}^{(i)}) - \boldsymbol{R}_{c.cas}(\boldsymbol{x}_{cas}^{(i)} + \boldsymbol{q}) \| \quad (7)$$

which reduces the misalignment between $\boldsymbol{R}_{c.cas}$ and $\boldsymbol{R}_{f.cas}$. The high-fidelity model of the cascade is evaluated at the beginning and end of each iteration i. Here, only one iteration of (5) is needed to satisfy the specs with $\boldsymbol{x}_{cas}^{*}$ = [0.14 0.14 0.12 3.89 0.42 1.04]^T mm, and l_{TL}^{*} = 3.34 mm.

The performance of the compact BLC developed using the proposed method is shown in Fig. 3(a). One can see a 40-MHz shift of the frequency characteristics and a non-ideal dS = 0.2 dB. This can be explained by the neglected T-junction effects. However, we can easily fine-tune the structure by means of a rapid design closure of [6]. By applying minor corrections given by $\Delta\boldsymbol{x}_{cas}$ = [0 0 0.01 0 0 –0.06]^T, perfect BLC performance is achieved, with a bandwidth of 31% and dS=0. The entire process together with design closure takes less than three evaluations of the high-fidelity BLC model, including direct optimization of the slow-wave cell (100 EM simulations of the cell at f_0, ~100 min of CPU time), direct optimization of the high-impedance branch (50 EM simulations of the branch at f_0, ~75 min of CPU time), construction of RSA models (13 EM simulations of the cell with adaptive frequency sweep, ~130 min, and 7 EM simulations of the branch with adaptive frequency sweep,

~105 min), two EM evaluations of the cascade using adaptive frequency sweep (at $\boldsymbol{x}_{cas}^{(0)}$ and $\boldsymbol{x}_{cas}^{*}$, ~100 mins), and two EM simulations of the entire BLC for the purpose of method numerical validation and final design fine-tuning (~50 hours). The estimated cost of direct optimization exploiting a high-fidelity EM model of the compact BLC is—approximately—150 EM simulations of the structure, which corresponds to 3750 hours of CPU time (~65 times longer than in case of the proposed approach). The final coupler shown in Fig.3(b) occupies 46.58 mm × 33.92 mm area, which is only 1/3 of the area of the reference device. The simulated values of $|S_{21}|$ and $|S_{31}|$ at f_0 are –3.089 dB and –3.089 dB, respectively. The phase difference between the output ports of the designed BLC is ~90.0° at f_0.

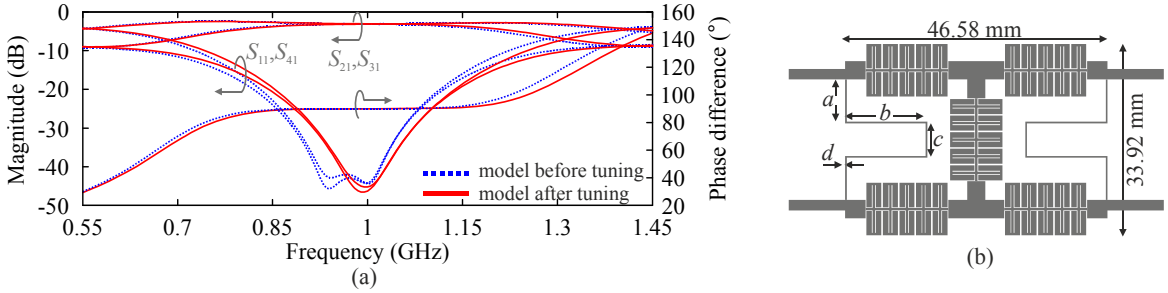

Fig. 3. (a) S-parameters of compact BLCs; (b) Layout of the designed coupler (a = 7.5 mm, b = 14.01 mm, c = 5.8 mm, d = 0.29 mm)

Conclusions

Simulated-driven design of a miniaturized branch-line coupler with a wideband operation has been investigated. Our approach exploits equivalent circuit models to discriminate between different realizations of slow-wave cells and establish apt repetition factor of the recurrent slow-wave structure. The presented surrogate-based optimization scheme has been tailored to handle design problems of multi-element slow-wave TLs with complex geometries.

***Authors**: Piotr Kurgan, Sławomir Kozieł, Gdańsk University of Technology, Faculty of Electronics, Telecommunications and Informatics, G. Narutowicza 11/12 str., 80-233 Gdańsk, Poland, E-mail: kurgan.piotr@gmail.com.*

REFERENCES

[1] Liao S.-S., Sun P.-T., Chin N.-C., Peng J.-T., A Novel Compact-Size Branch-Line Coupler, *IEEE Microw. Wireless Comp. Lett.,* vol. 15, (2005), no. 9, 588-590

[2] Chun Y.-H., Hong J.-S., Compact wide-band branch-line hybrids, *IEEE Trans. Microw. Theory Tech.,* vol. 54, (2006), no. 2, 704-709

[3] Kurgan P., Kitlinski M., Novel doubly perforated broadband microstrip branch-line couplers, *Microw. Opt. Tech. Lett.,* vol. 51, (2009), no. 9, 2149-2152

[4] Tseng C.-H., Wu C.-H., Design of compact branch-line couplers using π-equivalent artificial transmission lines, *IET Microw. Ant. Propag.,* vol. 6, (2012), no. 9, 969-974

[5] Kurgan P., Filipcewicz J., Kitlinski M., Development of a compact microstrip resonant cell aimed at efficient microwave component size reduction, *IET Microw. Ant. Propag.*, vol. 6, (2012), no. 12, 1291-1298

[6] Koziel S., Kurgan P., Rapid design of miniaturized branch-line couplers through concurrent cell optimization and surrogate-assisted fine-tuning, *IET Microw. Ant. Propag.*, vol. 9, (2015), no. 9, 957-963

[7] Seki S., Hasegawa H., Cross-tie slow-wave coplanar waveguide on semi-insulating GaAs substrates, *Electr. Lett.,* vol. 17, (1981), no. 17, 940-941

[8] Koziel S., Leifsson L. (Eds.), *Surrogate-based modeling and optimization. Applications in Engineering*, Springer, 2013

[9] Bandler J.W., Cheng Q.S., Dakroury S.A., Mohamed A.S., Bakr M.H., Madsen K., Sondergaard J., Space mapping: the state of the art, *IEEE Trans. Microw. Theory Tech.,* vol. 52, (2004), no. 1, 337-361

[10] Koziel S., Bekasiewicz A., Kurgan P., Rapid EM-Driven Design of Compact RF Circuits By Means of Nested Space Mapping, *IEEE Microw. Wireless Comp. Lett.,* vol. 24, (2014), no. 6, 364-366

[11] Mongia R., Bahl I., Bhartia P., RF and Microwave Coupled Line Circuits, Artech House, 1999

[12] Levy R., Lind L., Synthesis of symmetrical branch-guide directional couplers, *IEEE Trans. Microw. Theory Tech.,* vol. 16, (1968), no. 2, 80-89

[13] Ghali H., Moselhy T.A., Miniaturized Fractal Rat-Race, Branch-Line, and Coupled-Line Hybrids, *IEEE Trans. Microw. Theory Tech.,* vol. 52, (2004), no. 10, 2513-2520

[14] Agilent ADS, Agilent Technologies, 1400 Fountaingrove Parkway, Santa Rosa, CA 95403-1799, 2011

[15] Sonnet, version 14.54. Sonnet Software, North Syracuse, NY, US, 2013